Annals of Emerging Technologies in Computing (AETiC)
Vol. 9, No. 1, 2025

Research Article

Impact of Radial Grounding Model Granularity on Directivity of 433 MHz Monopole Antennas with Flat and Inclined Radials for ISM IoT Applications

Jinfeng Li[1,2,*] and Haolin Zhou[1]

[1]Beijing Institute of Technology, China
jinfengcambridge@bit.edu.cn; zhouhaolin@bit.edu.cn
[2]Imperial College London, United Kingdom
jinfengcambridge@bit.edu.cn
*Correspondence: jinfengcambridge@bit.edu.cn

Received: 28th November 2024; Accepted: 31st December 2024; Published: 1st January 2025

Abstract: Grounding is a critical factor in the performance of quarter-wave monopole antennas. Previous studies have explored finite, continuous grounding configurations with one- and two-dimensional variations in size for a 433 MHz vertical monopole antenna, identifying optimal geometries that maximize directivity while minimizing material costs and grounding size. However, these findings are not directly applicable to mission-critical environments (e.g., space, airborne, underwater, or ground-based applications) where continuous metallic grounding may be unavailable. This study extends the investigation to discretized grounding configurations, specifically employing radial monopoles formed by metal rods arranged in sparse or dense radial patterns. Both flat planar and inclined configurations of radial rods are analysed, with a focus on understanding the influence of design parameters, such as radial length and inclination angle, on antenna directivity and radiation patterns—key factors affecting signal reception in wireless communication systems, particularly in applications such as the internet of things (IoT). Using the Method of Moments (MoM) for simulation, the study provides practical guidelines for optimizing the design of 433 MHz monopole antennas constrained by finite and discrete grounding structures. The results indicate that an elevated radial configuration, consisting of five radials inclined at 5° from the monopole plane (equivalent to 85° from the horizontal plane) with a radial length of 2.5 meters, achieves a directivity of 9.23 dBi at 433 MHz. This represents a significant improvement over the flat planar configuration, which achieves a directivity of 6.23 dBi under the same conditions. These findings are particularly relevant for mobile communication, Internet of Things (IoT) devices, and radiofrequency (RF) systems requiring high performance from vertical monopole antennas in challenging grounding environments.

Keywords: ***Antenna directivity; Electromagnetics; Grounding in monopole antennas; Image theory; Internet of Things; ISM band; Radial monopole; 433 MHz***

1. Introduction

The frequency spectrum from 410 MHz to 6 GHz has been integral to Long-Term Evolution (LTE) for fourth-generation (4G) wireless communication [1,2] and the sub-6 GHz band for fifth-generation (5G) New Radio (NR) [3,4], underscoring its strategic significance in both historical and current communication systems. Within the lower frequency range, the 433 MHz band, allocated for industrial, scientific, and medical (ISM) applications [5,6], holds particular importance. In this band, quarter-wavelength vertical monopole antennas [7,8] serve as critical, compact front-end devices for wireless communication systems.

Jinfeng Li and Haolin Zhou, "Impact of Radial Grounding Model Granularity on Directivity of 433 MHz Monopole Antennas with Flat and Inclined Radials for ISM IoT Applications", *Annals of Emerging Technologies in Computing (AETiC)*, Print ISSN: 2516-0281, Online ISSN: 2516-029X, Vol. 9, No. 1, pp. 44-57, 1st January 2025, Published by International Association for Educators and Researchers (IAER), DOI: 10.33166/AETiC.2025.01.003, Available: http://aetic.theiaer.org/archive/v9/v9n1/p3.html.

The monopole antenna holds a significant place in the history of wireless communications, with its origins tracing back to the pioneering work of Guglielmo Marconi, often regarded as the father of wireless technology. Traditionally, the monopole antenna operates as a quarter-wavelength structure, with the height of the monopole above the ground plane serving as a critical design parameter. A key principle underlying its performance is image theory, which relies on the presence of an electrically large ground reference plane to create a mirror image of the radiating element, thereby enhancing its radiation properties. A comprehensive review of existing research on monopole antennas, including their theoretical foundations, can be found in [9,10]. Notably, the studies in [7] and [8] (our prior works) examine the critical role of ground planes, which electromagnetically replicate the other half of a dipole according to image theory [10,11]. These works investigate the performance metrics of a 433 MHz quarter-wavelength monopole antenna, such as gain, radiation patterns, voltage standing wave ratio (VSWR), and impedance matching. The analyses compare these metrics across various grounding configurations, including differences in material conductivity and geometries, specifically one-dimensional variations [7] and two-dimensional variations [8] in the sizes of the grounding planes.

It is important to note that the two foundational studies on the impact of monopole grounding were conducted using a continuous grounding plane with finite size and conductivity. In practical applications, particularly in constrained environments such as those found in Internet-of-Things (IoT) devices, the ideal continuous ground plane is often unavailable. In applications where continuous metallic grounding is unavailable (e.g., space, underwater, airborne, and ground-based scenarios), the insights derived from continuous grounding configurations are not directly applicable to discrete grounding structures for accurate performance prediction and informed decision-making. To address this limitation, a comprehensive investigation into discrete grounding configurations is essential. Discrete grounding offers potential advantages, including system miniaturization in terms of size, weight, and material cost. It is therefore crucial to explore the feasibility of replacing conventional continuous grounding planes with discrete or defected grounding structures. Specifically, the study must determine whether discrete configurations can achieve equivalent directivity or comparable gain without significant performance degradation. Addressing this research question and bridging the existing knowledge gap in the context of 433 MHz radial monopole antennas is of strategic importance for advancing antenna design in constrained environments.

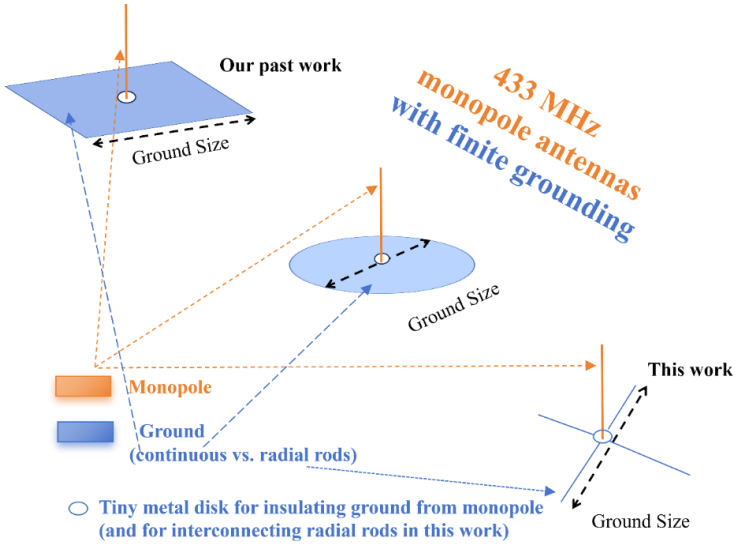

Figure 1. Evolution of 433 MHz vertically oriented monopole antenna designs, transitioning from continuous grounding (square, rectangular, circular) in previous works to discrete radial grounding in this work. Note that the vertical monopoles are insulated from both the continuous grounding planes and the discrete radial structures.

To address these limitations, radial ground configurations using discrete radial elements are employed. The performance of these configurations is influenced by several parameters, including the number and length of radial ground elements, the angle between radials, and their spacing relative to the monopole. Previous studies on the use of noncontinuous grounding solutions, such as radials [12,13], have primarily focused on frequencies in the low megahertz (MHz) range (e.g., 10 MHz [12]) or the

gigahertz (GHz) range [13]. However, there is a notable scarcity of research addressing the optimization of radial monopoles specifically for the 433 MHz Industrial, Scientific, and Medical (ISM) band, as defined by the International Telecommunication Union (ITU) and its Radio-Communication Sector (ITU-R). To address this gap, the present work investigates the performance of a 433 MHz vertical monopole antenna with radial grounding configurations, as illustrated in Figure 1. Radials, as a discrete alternative to continuous grounding planes, function analogously to meshes of a flat, continuous metallic plane, with the discrete elements interconnected via a small central metal disk, as depicted in Figure 1. The density of the radial rods, effectively forming the mesh, is determined by the number of radials employed (e.g., the example in Figure 1 shows a configuration with four radials). This study seeks to quantify the impact of these discrete grounding designs on antenna performance in the 433 MHz ISM band.

As illustrated in the three-dimensional (3D) models in Figure 2, this study employs the same monopole geometry as reported in our previous works on monopoles with continuous (but finite) grounding [7,8], specifically maintaining the vertical monopole height (H_{mono}) and the rod's cross-sectional size (W_{mono}). In this work, however, the grounding is replaced with a radial wire configuration, with key parameters including radial length (L_{radial}), radial width (W_{radial}), number of radials (N_{radial}), and angular spacing (θ_{radial}) between adjacent radial rods. It is important to note that the vertical monopole, extending from the feed, is electrically insulated from the grounding structure. The primary objective is to quantitatively compare the radiating performance of the radial monopole antenna with that of the conventional monopole antenna featuring continuous (but finite) grounding, particularly the optimized configurations from [7] (one-dimensional variation of the grounding size) and [8] (two-dimensional variation of the grounding size). In addition to the flat planar radial arrangement, Figure 2 also shows an elevated radial configuration, where the radial rods are inclined at an angle (α) relative to the vertical plane, with 90° representing the planar (horizontal) configuration.

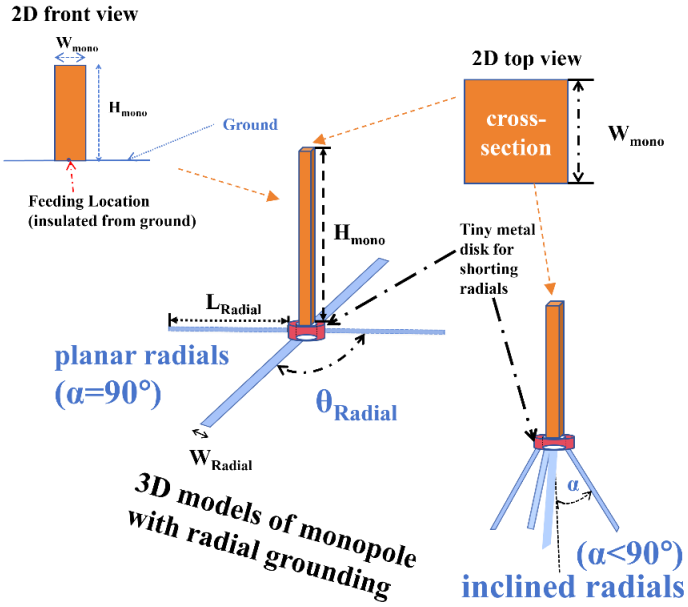

Figure 2. Depiction of 2D and 3D models of 433 MHz monopole antennas (centre-fed and electrically insulated from radial grounding rods, which are interconnected via a small metal disk). Two radial arrangements are considered and compared in this study: a planar distribution at ground level and an elevated configuration with inclined angles.

The paper is organized into six sections. Sections 2, 3, 4, and 5 present the variations in antenna directivity and radiation patterns (both 2D and 3D) as a function of the radial grounding parameters. The Method of Moments (MoM) [14,15] is used to solve the Green's Function [11] in free space, assuming all metallic components are perfect electric conductors (PEC). A summary of the workstation setup is provided in Table 1 below.

Table 1. Computational workstation setup supporting this study

Items	Details
CPU	AMD Ryzen Al 9 HX 370 w/Radeon 890M
GPU	NVIDIA GeForce RTX 4060 Laptop GPU GDDR6 @ 8 GB (128 bits)
Memory	32 GB LPDDR5X 7500 MHz

Specifically, Section 2 examines the impact of radial rod density (number of radials) in the planar grounding configuration. Section 3 explores the effect of radial length in the planar arrangement. Section 4 investigates the influence of tilting the radials at inclined angles, resulting in a sloping ground configuration. Section 5 extends the numerical investigations by varying the number of radials (from 4 to 32) and their lengths (from 0.05 m to 5 m, corresponding to 7.14λ), which presents a comprehensive analysis that integrates both two-dimensional and three-dimensional dependencies. This structured approach provides both theoretical and practical insights into the optimization of monopole antennas, with a focus on addressing the challenges posed by constrained grounding environments. Section 6 synthesizes these findings (continuous vs. discrete, planar vs. non-planar) to inform comprehensive decision-making, such as how to design a compact 433 MHz monopole antenna without compromising antenna gain. These insights provide valuable guidance for future research endeavors.

2. Impact of Radial Distribution Density on Antenna Directivity

In this section, we fix the radial length at L_{radial}=2 m (corresponding to a grounding size of 4 m, as determined in the continuous square-shaped grounding optimization study for the 433 MHz monopole [7]), while examining the effect of varying the number of discrete radial rods, i.e., parameterizing N_{radial} from 4 to 32, on the maximum directivity obtained from the 3D radiation pattern. Two distinct monopole cross-sectional designs are compared, as represented by the black and red curves in Figure 3. These designs are identical in terms of monopole rod height (following the quarter-wavelength principle), differing only in the cross-sectional sizes, specifically the W_{mono} for the square-shaped monopole rod. The black curve corresponds to the monopole rod with W_{mono}=0.0099 λ (the same size as the optimized design in [7]), while the red curve represents a thinner monopole rod with W_{mono}=0.0024 λ.

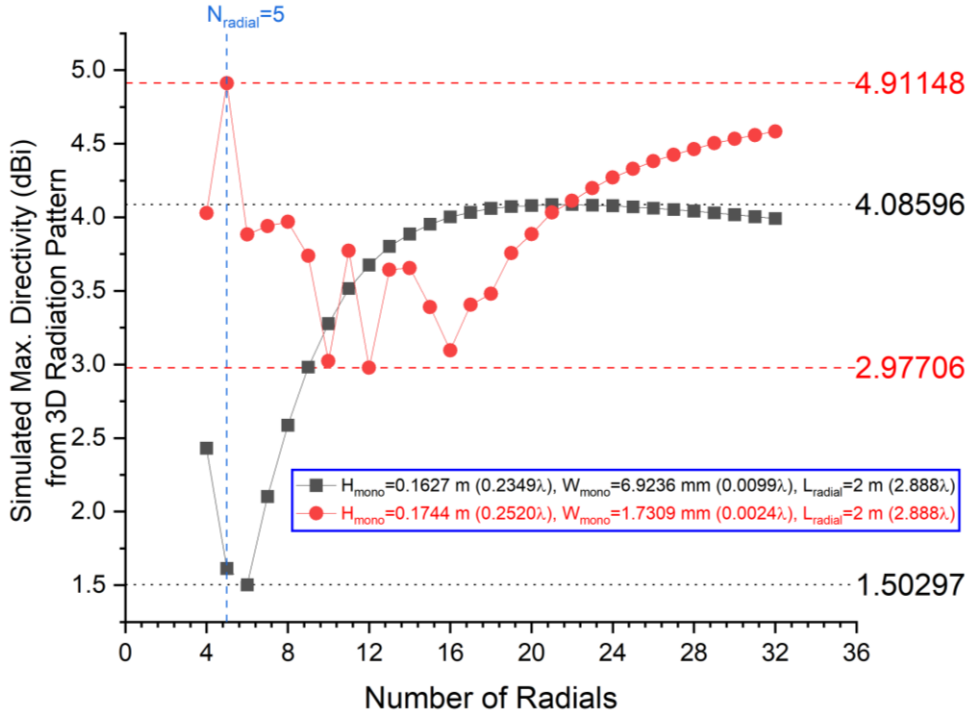

Figure 3. Simulated maximum directivity from the 3D radiation pattern as a function of the number of radial rods for two radial monopole designs with a grounding size of 4 m, differing in monopole cross-sectional sizes.

As shown in Figure 3, for the W_{mono}=0.0099 λ design, the maximum directivity generally increases with the number (density) of radials, leveling off at approximately N_{radial}=18, where the maximum directivity saturates at 4.08596 dBi. In contrast, for the W_{mono}=0.0024 λ design, a local maximum in directivity occurs earlier at N_{radial}=5, outperforming other radial configurations, although a similar increasing trend is observed from N_{radial}=16. In summary, the optimal number of radials for achieving the maximum directivity of 4.91148 dBi is 5.

3. Generalized Effect of Radial Length on Directivity and Radiation Patterns

In this section, we maintain the optimal number of radial rods (N_{radial}=5) for the W_{mono}=0.0024 λ monopole design and investigate the effect of radial length (L_{radial}) or grounding size ($2L_{radial}$) on radiation patterns and directivity. The results are compared with those obtained from a square-shaped grounding plane of the same size ($2L_{radial}$) and a circular grounding plane with a diameter of $2L_{radial}$. This comparison is conceptually significant, as illustrated in Figure 4 below, which shows the transition from continuous (square and circular) to discrete (radial rods) geometries in an area-reducing manner—first truncating the four edges of the square to form a circle, then removing most of the area from the circle to form radially distributed rods.

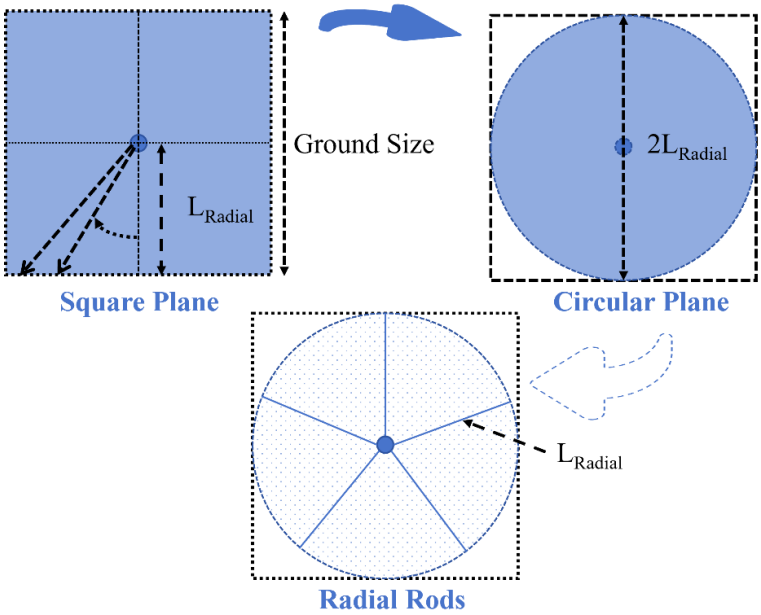

Figure 4. 2D top view illustrating the evolution of planar grounding from continuous square (asymmetric) to continuous circular (symmetric), and from circular (continuous) to radial (discrete).

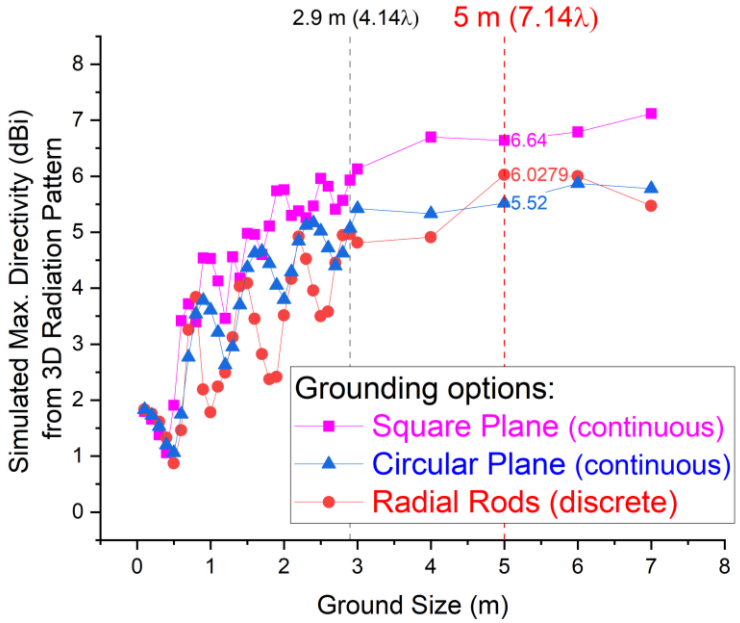

Figure 5. Maximum directivity of 3D radiation pattern parameterized with the grounding sizes of three grounding options (square plane, circular plane, and radial rods).

The L_{radial} in the square grounding configuration represents the shortest distance from the central feed point (where the vertical monopole is located) to the edge of the metal plane (ground). In other words, the benchmark for the asymmetric grounding geometry (i.e., the square grounding) is based on this shortest distance, defining the grounding size as $2L_{radial}$. In contrast, for the circular and radial grounding configurations, this consideration is unnecessary, as the geometries are symmetric in the

grounding plane, and the grounding size is consistently treated as $2L_{radial}$. The generalized results are presented in Figure 5, illustrating the grounding size parameterization ranging from 0.1 m to 7 m, which corresponds to a wavelength range from 0.14λ to 10λ.

Resultantly, the square-shaped grounding configuration (providing the largest grounding area for the feature size L_{radial}) yields the highest directivity, followed by the circular configuration, and then the radial one. This trend is exemplified by the grounding size of 2.9 m (L_{radial}=1.45 m), corresponding to 4.14λ. The difference in achievable directivity can be attributed to the grounding area, with square > circular > radial in terms of performance. Notably, at a grounding size of 5 m (7.14λ) with L_{radial}=2.5 m, the radial design (6.0279 dBi) outperforms the circular grounding design (5.52 dBi). To provide a broader perspective on the radiation patterns in both 3D and 2D (azimuth angle of 0°, abbreviated as az = 0°), Figures 6 and 7 present the results for the grounding sizes of 2.9 m and 5 m, respectively.

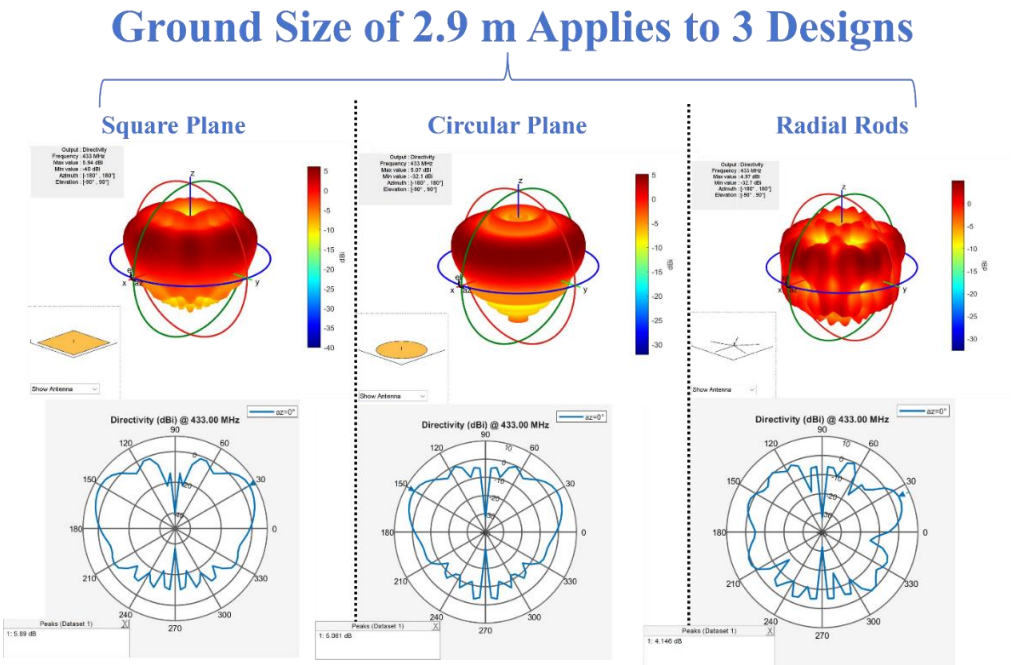

Figure 6. Maximum directivity derived from 3D and 2D (az = 0°) radiation patterns of three monopole antenna designs at 433 MHz with a grounding size of 2.9 m, comparing square plane, circular plane, and radial configurations.

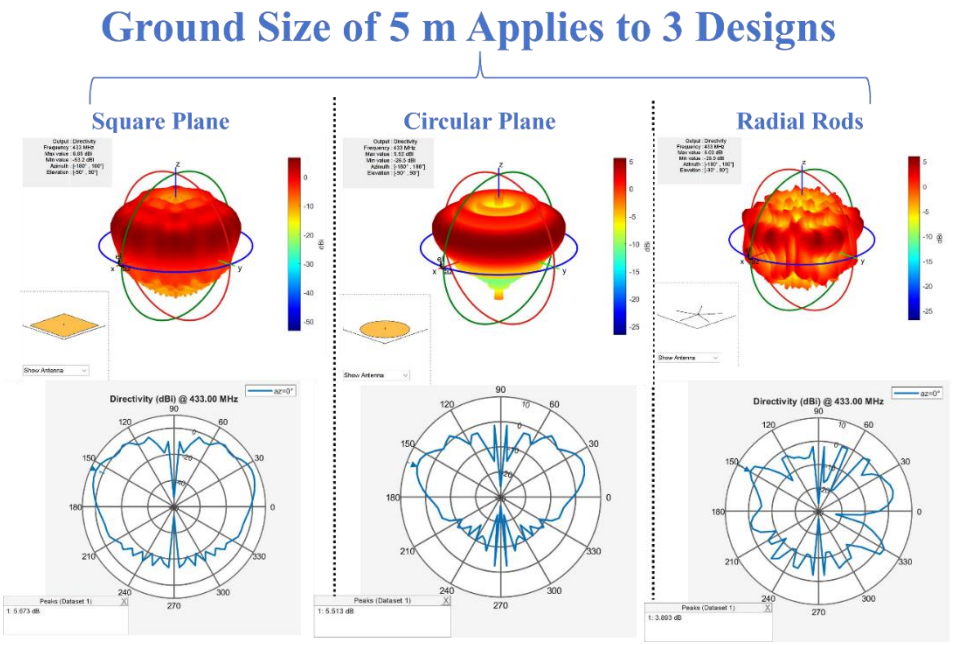

Figure 7. Maximum directivity derived from 3D and 2D (az = 0°) radiation patterns of three monopole antenna designs at 433 MHz with a grounding size of 5 m, comparing square plane, circular plane, and radial configurations.

4. Impact of Elevated Radial Inclination on Directivity and Radiation Patterns

While the sources of directivity improvement can vary—such as by increasing the metallic grounding area or deploying antenna arrays—these conventional methods often require additional space and incur higher costs. In this section, we explore a vertically tilted approach for arranging the radial rods, as illustrated in Figure 2. The optimized values of N_{radial}=5 (from Section 2) and L_{radial} =2.5 m (from Section 3) are fixed, while the vertical tilt angle α (shown in Figure 8) is varied from 90° (representing the planar solution analyzed in Sections 2 and 3) to 0° (vertical alignment with the monopole). The results are presented in Figure 9, where 90° – α represents the tilting angle relative to the horizontal plane.

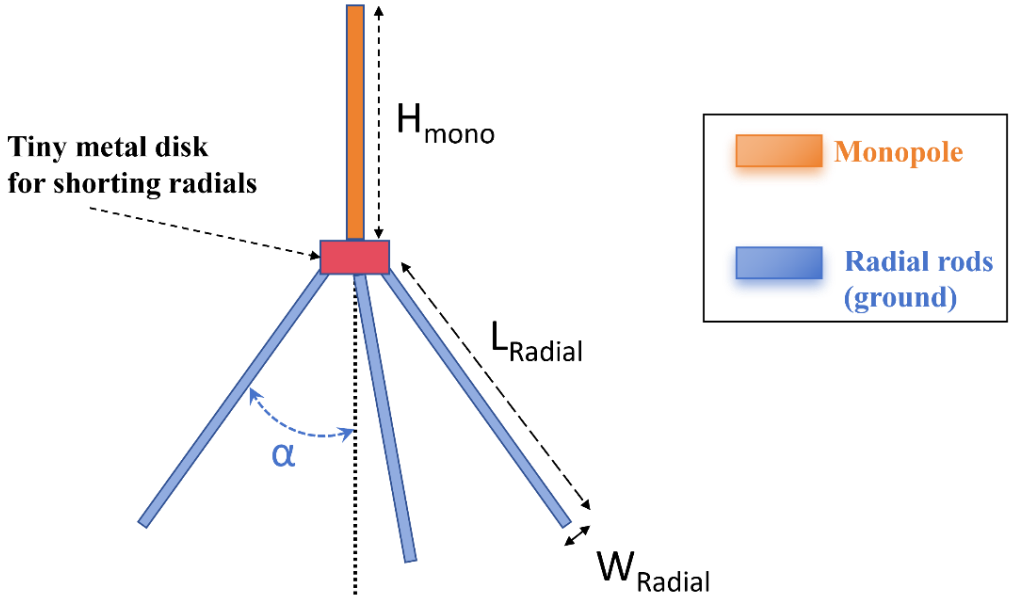

Figure 8. Schematic of vertically angled radials with an inclination of α degrees from the vertical plane.

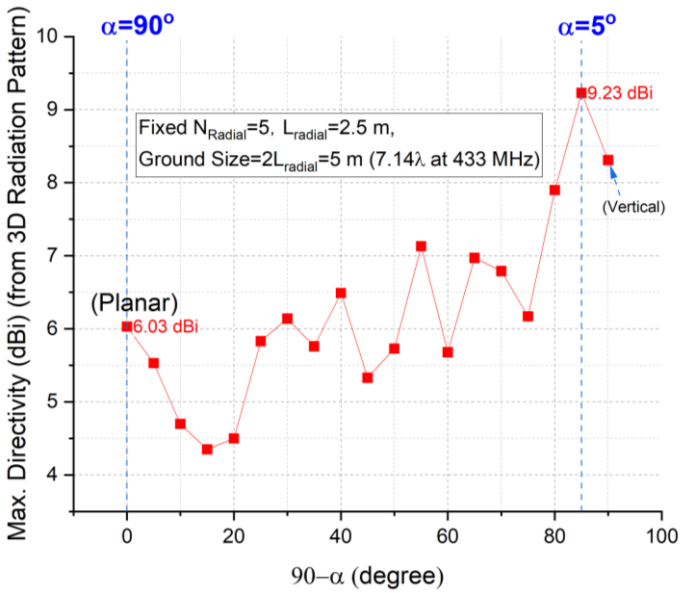

Figure 9. Directivity enhancement through vertically angled radials (α degrees from the vertical plane) at 433 MHz.

As demonstrated by the numerical results in Figure 9, tilting the radials away from the vertical plane by 5° leads to a significant improvement in antenna directivity, increasing from 6.03 dBi (for the optimized planar design from Sections 2 and 3) to 9.23 dBi (with a 5° tilt from the vertical plane, or 85° from the horizontal plane). This enhancement in directivity mimics the behaviour of an antenna array, despite the fact that only a standalone monopole with vertically angled radials is used. This elevated radial grounding configuration provides an opportunity to optimize a compact and simple monopole

antenna without the need for arrays. To further support these findings, Figure 10 presents the 3D and 2D radiation patterns for two radial grounding configurations: one with a planar (non-tilted) arrangement and the other with an 85° tilt angle from the horizontal plane.

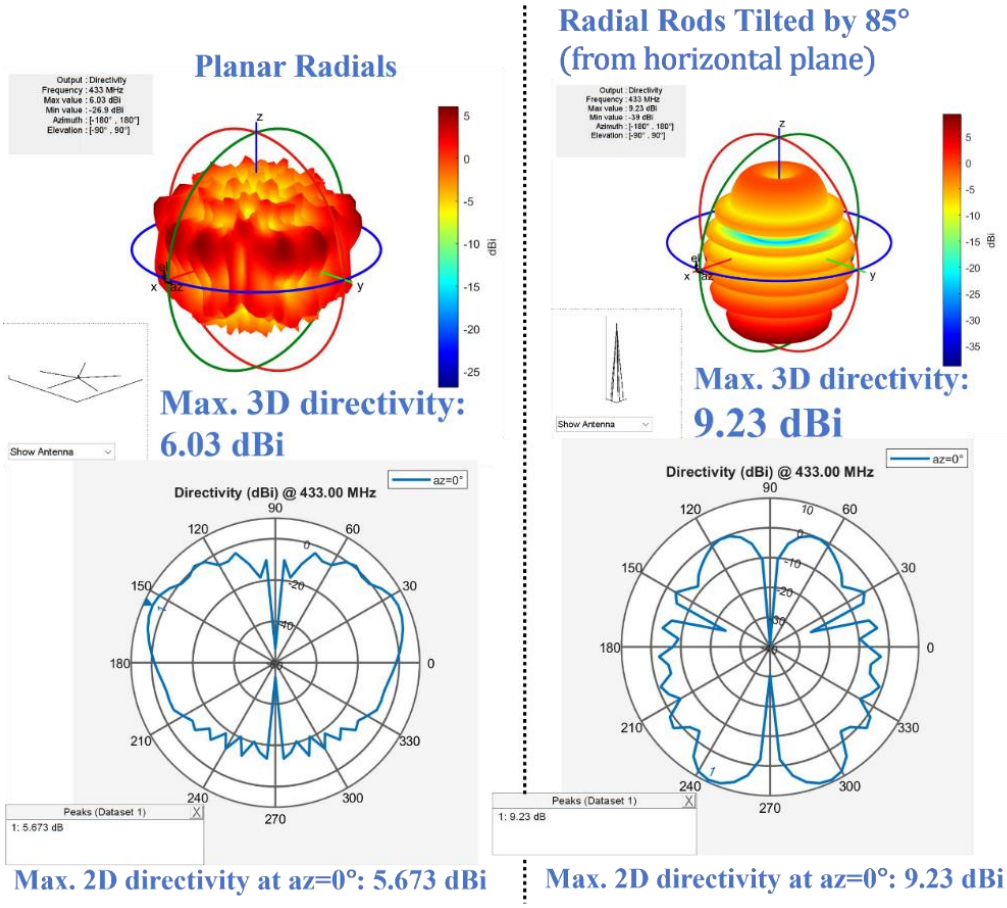

Figure 10. 3D and 2D (az = 0°) radiation patterns of two radial monopole antenna designs at 433 MHz. Both designs use 5 radial rods with a radial length of 2.5 m, differing in tilting angles from the horizontal plane.

5. Summary and Optimizations

To summarize, the study formulates the evaluation of monopole antenna performance as an engineering optimization problem, focusing on maximizing directivity D_{max} under varying configurations of radial ground elements. The analysis is conducted using 3D radiation patterns, encompassing both azimuth and elevation planes, and the vertically aligned angle α is parameterized from 0° to 90° to represent the transition from the horizontal to the vertical plane. As shown in Figure 11, the value of D_{max} depends significantly on α, ranging from 4.35 dBi at α=75° (worst case) to 9.23 dBi at α=5° (optimum case). These observations serve as the basis for further analysis of the effects of radial configurations.

To ensure consistency in the evaluation, the monopole dimensions are fixed at H_{mono} of 0.17448 m (0.2520λ) and W_{mono} of 0.0017309 m (0.0024λ). The investigation explores the influence of two key parameters, i.e., the radial length (L_{radial}), and the number of radials (N_{radial}). To capture the dependency of D_{max} on these parameters, two specific tilting scenarios are analysed: (1) Optimal tilting angle (α=5°): Associated with the maximum directivity based on Figure 11; and (2) Worst-case tilting angle (α=75°): Representing the lower boundary of performance.

The computations are performed using MATLAB, with customized scripts to automate the parameterization and evaluation of radial configurations. Figure 12 illustrates the MATLAB code snippet employed for the case of α=5°, where radial lengths and numbers are systematically varied, and D_{max} is computed from the corresponding 3D radiation patterns. The results obtained for these configurations are analysed to uncover trends and establish insights into the impact of radial length and radial number on directivity. This systematic approach provides a robust framework for optimizing monopole antenna designs, especially for constrained environments commonly encountered in IoT applications.

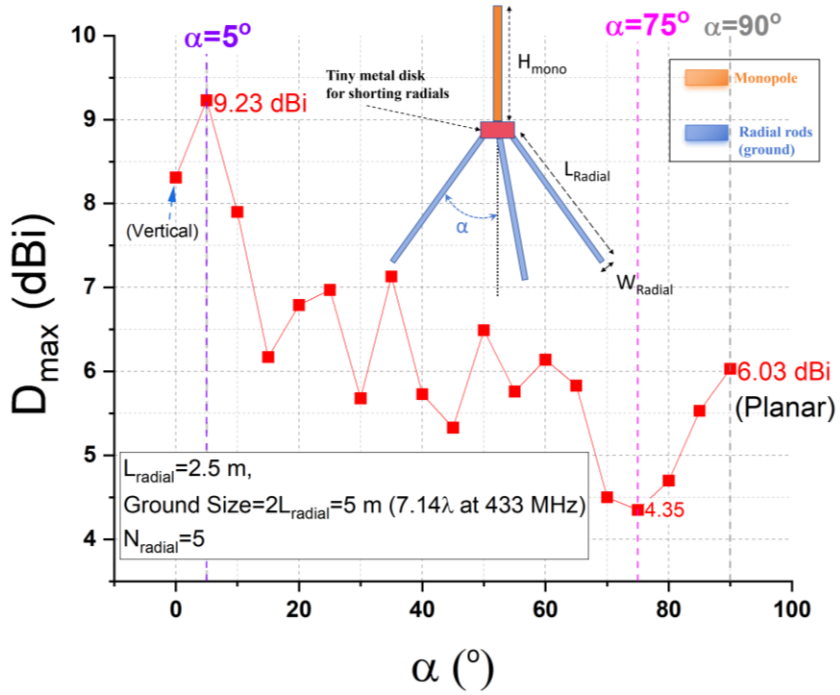

Figure 11. Quantification of the dependency of D_{max} on radial tilting angle α (results adapted from Figure 9).

```
% 433 MHz ISM band operation
frequency = 433e6;

% define the parameterization range of radial grounding geometry
numRadialsRange = 4:32; % number of radials varying from 4 to 32
radialLengthRange = 1.5:0.5:5; % radial length varying from 1.5 m to 5 m with spacing of 0.5 m

% calculate matrix dimensions
numRadials = length(numRadialsRange);
numLengths = length(radialLengthRange);

% initialize maximum directivity matrix
maxDirectivityMatrix = zeros(numRadials, numLengths);

% create progress bar
h = waitbar(0, 'Please wait...');

% traversal of radial geometry (number of radials and length of radials)
for i = 1:numRadials
    for j = 1:numLengths
        % update progress bar
        waitbar(i + (j-1)/numLengths*numRadials, h, sprintf('Processing radials %d, length %0.2f',
numRadialsRange(i), radialLengthRange(j)));

        % radial ground with tilted angle of 85 degree away from the horizontal plane
        antennaObject = design(monopoleRadial, frequency);
        antennaObject.NumRadials = numRadialsRange(i);
        antennaObject.RadialLength = radialLengthRange(j);
        antennaObject.RadialTilt = 85;

        % calculate maximum directivity
        D = pattern(antennaObject, frequency);
        maxDirectivity = max(D(:));

        % record maximum directivity
        maxDirectivityMatrix(i, j) = maxDirectivity;
    end
end

% close the progress bar
close(h);

% display the maximum directional matrix
disp(maxDirectivityMatrix);
```

Figure 12. MATLAB code for the multi-dependency study (a partial range of parameterization is illustrated).

The numerical analysis reveals the intricate relationship between the maximum directivity (D_{max}) of the monopole antenna and two key design parameters: the length of the radial ground elements (L_{radial}) and the number of radial elements (N_{radial}).

As illustrated in Figure 13, directivity increases consistently with both the number and length of radial elements, confirming the theoretical expectation that larger and more numerous radials improve the antenna's radiation efficiency. Specifically: (1) Radial length (L_{radial}): Directivity improves as L_{radial} approaches an optimal value, typically near four wavelengths (4λ). Beyond this range, the behaviour becomes more complex and non-monotonic (saturated), as shown by the two-dimensional contour in Figure 14. This suggests that overly long radials introduce interference effects or other structural inconsistencies that counteract the expected gains; (2) Number of radials (N_{radial}): Increasing N_{radial} enhances D_{max}, although the marginal improvement diminishes as the number exceeds a practical threshold (e.g., beyond 24 radials).

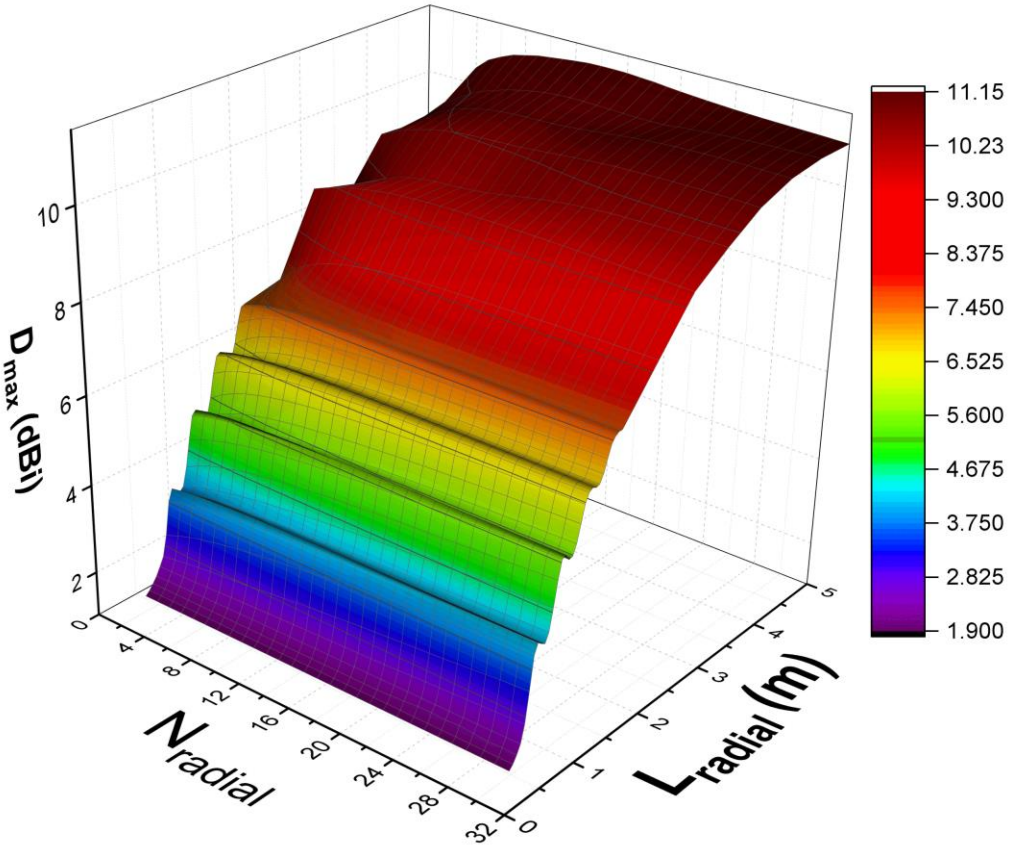

Figure 13. Maximum directivity (D_{max}) of various radial conditions under α=5°: D_{max} vs. N_{radial} and L_{radial} (in meters).

This 3D visualization highlights the trade-offs in monopole antenna design. While longer radials and a greater number of radials generally lead to better directivity, practical limitations such as material costs, fabrication complexity, and spatial constraints necessitate careful optimization. For this study, N_{radial} was varied from 4 to 32, and L_{radial} was parameterized from 0.07143λ to 7.14λ (0.05 m to 5 m). The resulting 3D plots (Figure 13) and 2D contour (Figure 14) provide valuable insights into the multidimensional dependencies of D_{max}, offering a comprehensive perspective for antenna optimization in constrained environments.

To expand the results' comparison with another tilting angle (α=75°), Figure 15 below illustrates the results of α=5° and α=75° in the same graph, both are parameterizing with the radial numbers and radial lengths. To validate these findings, prototypes of radial monopole antennas are being manufactured using advanced fabrication techniques, including 3D printing [16] and CNC machining [17]. The prototypes will undergo experimental testing in an anechoic chamber [18], where the radiation patterns and far-field characteristics will be characterized using network analysers [19]. This validation process will ensure the reliability and applicability of the simulation results to real-world IoT applications [20].

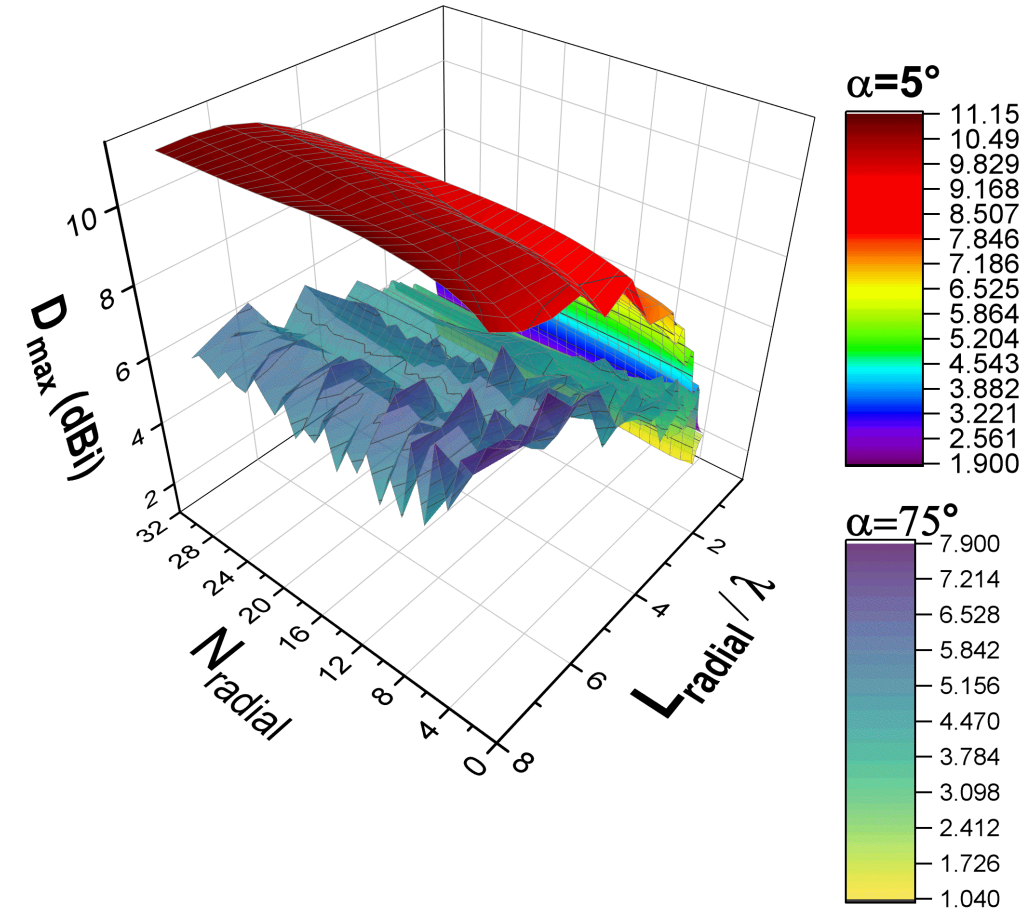

Figure 14. Maximum directivity (D_{max}) of various radial conditions under α=5°: D_{max} vs. N_{radial} and the electrical length of L_{radial}/λ.

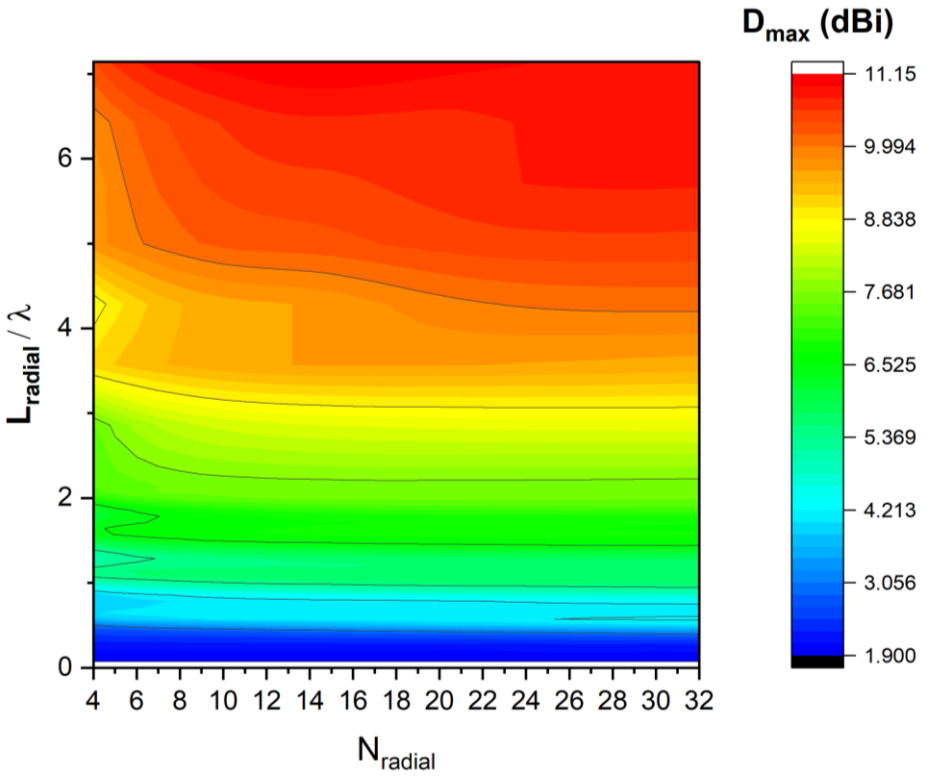

Figure 15. Comparative study of α=5° and α=75° for radial geometry parameterization.

6. Discussions and Conclusions

While advancements in wireless communication protocols are driving operating frequencies higher, from microwave to millimeter-wave and beyond (into terahertz and optical ranges), the 433 MHz ISM band remains critically important for Internet-of-Things (IoT) applications. This is primarily due to its ability to provide long-range coverage with cost-effective solutions. A fundamental component enabling 433 MHz IoT is the antenna, particularly the quarter-wavelength monopole antenna, which traditionally relies on an electrically large metal grounding plane for effective operation based on image theory. However, most IoT devices operate in constrained environments, often lacking a continuous grounding plane. To address this limitation, the grounding structure must be adaptable and optimized for practical applications.

This paper presents a comprehensive evaluation of 433 MHz monopole antennas with radial grounding solutions, focusing on the dependence of maximum directivity on the number of flat radials (Section 2), the length of the flat radials (Section 3), and the inclined angles of the sloping radials (Section 4). The numerical results for maximum directivity and radiation patterns (both 3D and 2D) are benchmarked against continuous grounding solutions of varying shapes (square and circular, representing asymmetric and symmetric configurations, respectively). This comparison helps elucidate the nonlinear behaviour of the grounding area's impact (relative to the guided wavelength) on monopole antenna performance. The optimized 433 MHz radial monopole antenna features 5 radial rods, each 2.5 m in length (forming a discrete grounding size of 5 m or 7.14 λ), with an 85° tilt from the horizontal plane. This configuration achieves a maximum directivity of 9.23 dBi at 433 MHz, representing a substantial improvement in signal reception compared to the non-tilted radial solution (6.03 dBi), the square-plane solution (6.64 dBi), and the circular-plane solution (5.52 dBi). Section 5 systematically analyses the effects of simultaneously varying radial number (4 to 32) and radial length (0 to 5 m, corresponding to 7.14λ). The investigation explores both two-dimensional (2D) and three-dimensional (3D) aspects of the problem, providing insights into performance optimization under constrained grounding conditions.

Building upon these findings, future research will focus on further optimizing the radial monopole antenna design by exploring additional parameters beyond radial length, number, and tilting angles. Specifically, the influence of material properties and environmental factors on antenna performance will be investigated. Furthermore, the practical applicability of the proposed design in real-world communication systems will be assessed experimentally, particularly its integration into mobile, IoT, and other wireless technologies. In addition, future work will aim to reduce the overall antenna size while maintaining high performance, potentially through the use of advanced materials [21] or hybrid grounding configurations, to further enhance directivity and radiation efficiency.

Acknowledgement

The authors thank the support from the National Natural Science Foundation of China under Grant 62301043, and the Fundamental Research Funds for the Central Universities (Beijing Institute of Technology Research Fund Program for Young Scholars).

References

[1] Ian F. Akyildiz, David M. Gutierrez-Estevez, Ravikumar Balakrishnan and Elias Chavarria-Reyes, "LTE-Advanced and the evolution to Beyond 4G (B4G) systems", *Physical Communication*, ISSN 1874-4907, Vol. 10, pp. 31-60, March 2014, Published by Elsevier B.V., DOI: 10.1016/j.phycom.2013.11.009, Available: https://www.sciencedirect.com/science/article/pii/S1874490713000864.

[2] Peter S. Excell, "The British Electronics and Computing Industries: Past, Present and Future", *Annals of Emerging Technologies in Computing (AETiC)*, Print ISSN: 2516-0281, Online ISSN: 2516-029X, Vol. 2, No. 3, pp. 45-52, July 2018, United Kingdom, Published by International Association for Educators and Researchers (IAER), DOI: 10.33166/AETiC.2018.03.005, Available: https://aetic.theiaer.org/archive/v2/v2n3/p5.html.

[3] Utkarsh Pandey, Parulpreet Singh, Raghvendra Singh, Vivek Kumar, Kanad Ray *et al.*, "Ultra-wideband microstrip folded antenna for wireless LAN, 5G and Internet of Things applications", *Scientific Reports*, Online ISSN: 2045-2322, Vol. 14, 29319, November 2024, Published by Springer Nature, DOI: 10.1038/s41598-024-65502-6, Available: https://www.nature.com/articles/s41598-024-65502-6.

[4] Jinfeng Li, "Optically steerable phased array enabling technology based on mesogenic azobenzene liquid crystals for starlink towards 6G", in *Proceedings of the 2020 IEEE Asia-Pacific Microwave Conference (APMC)*, 08-11 December 2020, Hong Kong, Electronic ISBN: 978-1-7281-6962-0, pp. 345-347, Published by IEEE, DOI: 10.1109/APMC47863.2020.9331345, Available: https://ieeexplore.ieee.org/document/9331345.

[5] Musa Hussain, Anees Abbas, Wahaj A. Awan and Syeda I. Naqvi, "Miniaturized Arrow-Shaped Flexible Filter-Embedded Antenna for Industrial and Medical Applications", *Applied Sciences*, ISSN: 2076-3417, Vol. 14, No. 23, 11004, November 2024, Published by MDPI, DOI: 10.3390/app142311004, Available: https://www.mdpi.com/2076-3417/14/23/11004.

[6] Deepti Sharma, Rakesh N. Tiwari, Sachin Kumar, Satyendra Sharma and Ladislau Matekovits, "A Compact Wearable Textile Antenna for NB-IoT and ISM Band Patient Tracking Applications", *Sensors*, ISSN: 1424-8220, Vol. 24, No. 15, 5077, August 2024, Published by MDPI, DOI: 10.3390/s24155077, Available: https://www.mdpi.com/1424-8220/24/15/5077.

[7] Jinfeng Li, "Performance Limits of 433 MHz Quarter-wave Monopole Antennas due to Grounding Dimension and Conductivity", *Annals of Emerging Technologies in Computing (AETiC)*, Print ISSN: 2516-0281, Online ISSN: 2516-029X, Vol. 6, No. 3, pp. 1-10, July 2022, Published by International Association for Educators and Researchers, DOI: 10.33166/AETiC.2022.03.001, Available: https://aetic.theiaer.org/archive/v6/v6n3/p1.html.

[8] Jinfeng Li, "Demystifying Two-Dimensional Asymmetrical Grounding Impacts on Monopole Antennas at 433 MHz", in *Proceedings of the 9th IEEE International Conference on Microwaves, Communications, Antennas, Biomedical Engineering and Electronic Systems (IEEE COMCAS 2024)*, 09-11 July 2024, Tel Aviv, Israel, Electronic ISBN: 979-8-3503-4818-7, Electronic ISSN: 2150-8968, pp. 1–4, Published by IEEE, DOI: 10.1109/COMCAS58210.2024.10666235, Available: https://ieeexplore.ieee.org/document/10666235.

[9] J. S. Belrose, "Vertical monopoles with elevated radials: an up-date", in *Proceedings of the Tenth International Conference on Antennas and Propagation*, 14-17 April 1997, Edinburgh, UK, Print ISBN: 0-85296-686-5, Print ISSN: 0537-9989, Vol. 1, pp. 190-195, Published by IEEE, DOI: 10.1049/cp:19970236, Available: https://ieeexplore.ieee.org/document/608547.

[10] Hanieh Aliakbari and Buon K. Lau, "Characteristic Mode Analysis of Planar Dipole Antennas", in *Proceedings of the 2019 13th European Conference on Antennas and Propagation (EuCAP)*, 31 March 2019 - 05 April 2019, Krakow, Poland, Electronic ISBN: 978-88-907018-8-7, pp. 1-5, Published by IEEE, Available: https://ieeexplore.ieee.org/document/8739305.

[11] Salma Mirhadi, Mohammad Soleimani and Ali Abdolali, "Analysis of finite ground plane effects on antenna performance using discrete Green's function", in *Proceedings of the 2012 15 International Symposium on Antenna Technology and Applied Electromagnetics*, 25-28 June 2012, Toulouse, France, Electronic ISBN: 978-1-4673-0292-0, Print ISBN: 978-1-4673-0290-6, pp. 1-3, Published by IEEE, DOI: 10.1109/ANTEM.2012.6262332, Available: https://ieeexplore.ieee.org/document/6262332.

[12] Mahdi Fartookzadeh, Seyyed H.M. Armaki, Seyyed M.J. Razavi and Jalil R. Mohassel, "Optimum Functions for Radial Wires of Monopole Antennas with Arbitrary Elevation Angles", *Radioengineering*, Print ISSN: 1210-2512, Vol. 25, No. 1, pp. 53-60, April 2016, Published by Czech and Slovak Technical Universities, DOI: 10.13164/re.2016.0053, Available: https://www.radioeng.cz/fulltexts/2016/16_01_0053_0060.pdf.

[13] Bing Wang, Zhongxiang Shen, Theng H. Gan and Yee H. Lee, "Radiation Pattern Improvement of a Wide-Band Planar Monopole Antenna", in *Proceedings of the 2024 IEEE International Symposium on Antennas and Propagation and INC/USNC-URSI Radio Science Meeting (AP-S/INC-USNC-URSI)*, 14-19 July 2024, Firenze, Italy, Electronic ISSN: 1947-1491, pp. 2219-2220, Published by IEEE, DOI: 10.1109/AP-S/INC-USNC-URSI52054.2024.10686352, Available: https://ieeexplore.ieee.org/document/10686352.

[14] Yuehe Ge and K. P. Esselle, "A fast method of moments based on a new closed-form Green's function for microstrip structures", in *Proceedings of the IEEE Antennas and Propagation Society International Symposium, 2001 Digest, Held in conjunction with: USNC/URSI National Radio Science Meeting*, Print ISBN: 0-7803-7070-8, 08-13 July 2001, Boston, MA, USA, pp. 794-797, Published by IEEE, DOI: 10.1109/APS.2001.959843, Available: https://ieeexplore.ieee.org/document/959843.

[15] B. J. Fasenfest, F. Capolino, D. R. Wilton, D. R. Jackson and N. J. Champagne, "A fast MoM solution for large arrays: Green's function interpolation with FFT", *IEEE Antennas and Wireless Propagation Letters*, Print ISSN: 1536-1225, Electronic ISSN: 1548-5757, Vol. 3, pp. 161-164, 31 December 2004, Published by IEEE, DOI: 10.1109/LAWP.2004.833713, Available: https://ieeexplore.ieee.org/document/1324094.

[16] Kevin M.K.H. Leong, Evan Nguyen, Jesse Tice and Vesna Radisic, "3D Printed Folded Monopole Antennas", in *Proceedings of the 2023 IEEE International Symposium on Antennas and Propagation and USNC-URSI Radio Science Meeting (USNC-URSI)*, 23-28 July 2023, Portland, OR, USA, Electronic ISBN: 978-1-6654-4228-2, Electronic ISSN: 1947-1491, pp. 1081-1082, Published by IEEE, DOI: 10.1109/USNC-URSI52151.2023.10238205, Available: https://ieeexplore.ieee.org/document/10238205.

[17] Dipankar Sutradhar, Durlav Hazarika and Sunandan Bhunia, "Design of Small-Sized Meander Lined Printed Monopole Antenna Operating in VHF Range", *Lecture Notes in Networks and Systems*, Print ISBN: 978-981-16-1394-

4, Online ISBN: 978-981-16-1395-1, Vol. 204, pp. 517-525, 08 June 2021, Published by Springer, Singapore, DOI: 10.1007/978-981-16-1395-1_38, Available: https://link.springer.com/chapter/10.1007/978-981-16-1395-1_38.

[18] George V. R. Xavier, Edson G. da Costa, Alexandre J. R. Serres, Luiz A. M. M. Nobrega, Adriano C. Oliveira *et al.*, "Design and Application of a Circular Printed Monopole Antenna in Partial Discharge Detection", *IEEE Sensors Journal*, Print ISSN: 1530-437X, Electronic ISSN: 1558-1748, Vol. 19, No. 10, pp. 3718-3725, 31 January 2019, Published by IEEE, DOI: 10.1109/JSEN.2019.2896580, Available: https://ieeexplore.ieee.org/document/8631122.

[19] M. D. Migliore and D. Pinchera, "A network-analyser calibration method for accurate measurement of the reflection coefficients of monopolelike antennas", *Microwave and Optical Technology Letters*, Online ISSN: 1098-2760, Print ISSN: 0895-2477, Vol. 47, No. 4, pp. 330-332. 26 September 2005, Published by John Wiley & Sons, DOI: 10.1002/mop.21161, Available: https://onlinelibrary.wiley.com/doi/10.1002/mop.21161.

[20] Jinfeng Li and Haorong Li, "Computationally Sampling Surface and Volume Current Densities of Liquid Crystal Non-Planar Phase Shifters for Low-Loss 5G IoT and 6G AIoT", in *Proceedings of the 2024 IEEE International Conference on Omni-layer Intelligent Systems (COINS)*, 29-31 July 2024, London, United Kingdom, Electronic ISBN: 979-8-3503-4959-7, Electronic ISSN: 2996-5330, pp. 1-6, Published by IEEE, DOI: 10.1109/COINS61597.2024.10622149, Available: https://ieeexplore.ieee.org/document/10622149.

[21] A. Kabalan, A. C. Tarot and A. Sharaiha, "Miniaturization of a broadband monopole antenna using low loss magneto-dielectric materials in VHF band", in *Proceedings of the Loughborough Antennas & Propagation Conference (LAPC 2017)*, 13-14 November 2017, Loughborough, United Kingdom, Electronic ISBN: 978-1-78561-700-3, Print ISBN: 978-1-78561-699-0, pp. 1-4, Published by Institution of Engineering and Technology (IET), DOI: 10.1049/cp.2017.0303, Available: https://ieeexplore.ieee.org/document/8364415.